Bioorganic & Medicinal Chemistry Letters 19 (2009) 1177–1182

Contents lists available at ScienceDirect

Bioorganic & Medicinal Chemistry Letters

journal homepage: www.elsevier.com/locate/bmcl

Anthranilimide based glycogen phosphorylase inhibitors for the treatment of type 2 diabetes. Part 3: X-ray crystallographic characterization, core and urea optimization and in vivo efficacy

Stephen A. Thomson *, Pierette Banker, D. Mark Bickett, Joyce A. Boucheron, H. Luke Carter, Daphne C. Clancy, Joel P. Cooper, Scott H. Dickerson, Dulce M. Garrido, Robert T. Nolte, Andrew J. Peat, Lauren R. Sheckler, Steven M. Sparks, Francis X. Tavares, Liping Wang, Tony Y. Wang, James E. Weiel

Metabolic Center for Excellence in Drug Discovery, GlaxoSmithKline, 5 Moore Drive, PO Box 13398, Research Triangle Park, NC 27705, USA

ARTICLE INFO

Article history:
Received 9 October 2008
Revised 17 December 2008
Accepted 19 December 2008
Available online 25 December 2008

Keywords:
Glycogen
Phosphorylase
Inhibitor
Anthranilimide
Glucagon
Challenge
Antidiabetic

ABSTRACT

Key binding interactions of the anthranilimide based glycogen phosphorylase *a* (GPa) inhibitor **2** from X-ray crystallography studies are described. This series of compounds bind to the AMP site of GP. Using the binding information the core and the phenyl urea moieties were optimized. This work culminated in the identification of compounds with single nanomolar potency as well as in vivo efficacy in a diabetic model.

Type 2 diabetes has reached near epidemic proportions in most of the developed world and results in acute and chronic complications, disability, and death. The degree of this problem is exemplified in the fact that type 2 diabetes is now becoming prevalent in children and adolescents.[1] An increase in the prevalence and degree of obesity in children is a likely driver of the increase in type 2 diabetes in this population.[2] Although there are several treatment options for type 2 diabetes, long term efficacy of oral antidiabetic agents has been limited. It has recently been reported that 21% of patients will fail on metformin treatment within 5 years.[3] Therefore new treatment options are needed that can either be used as mono-therapy or in combination with other agents. Excessive hepatic glucose production is a major component of hyperglycemia and consists of both glycogenolysis and gluconeogenesis. In the postprandial state glycogenolysis was increased more than twofold in diabetic subjects compared to non-diabetics. In addition diabetics have a 55% reduction in liver glycogen content compared to normal subjects.[4] The enzyme glycogen phosphorylase *a* (GPa) is responsible for the release of glucose-1-phosphate from glycogen and is the rate determining step in glycogenolysis. GPa has therefore become a target for glucose lowering in type 2 diabetes. Although several groups have reported small molecule inhibitors of GPa, definitive clinical results have not been communicated.[5]

In previous papers, we have outlined some of the properties and SAR of a novel anthranilimide series of GPa inhibitors exemplified by compound **1**.[6]

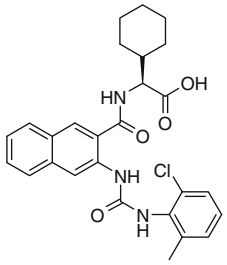

1

IC_{50} = 73 nM
IC_{50} (cell) =600 nM
CYP2C9 IC_{50} = 1000 nM

* Corresponding author.
E-mail address: stephen.a.thomson@gsk.com (S.A. Thomson).

0960-894X/$ - see front matter © 2009 Elsevier Ltd. All rights reserved.
doi:10.1016/j.bmcl.2008.12.085

We have reported on the SAR of the amino-acid head group and how modification at this position can affect the potency of CYP450 inhibition.[7] Overall low nanomolar potency for GPa inhibition and decreased P450 inhibition can be obtained by replacement of the cyclohexyl containing amino-acid head group with a *t*-butyl threonine head group. In addition replacement of the 2-methyl-6-chloro phenyl group of **1** with a 2,4,6-trimethylphenyl group improved potency as well, giving compound **2**.

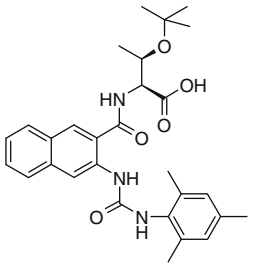

2
IC_{50} = 7 nM
IC_{50} (cell) =139 nM
CYP2C9 IC_{50} = 10000 nM

One concern with compound **2** is the potential to form reactive metabolites via the known pathway of epoxidation across the 5,6 or 7,8 positions of the naphthalene ring system.[8] Indeed incubation of compound **2** with human liver microsomes in the presence of glutathione and analysis by LC/MS/MS gave ions consistent with such a process occurring.[9] In light of this result and the desire to further understand the SAR of this series of compounds, we investigated replacements to the naphthalene ring system and explored the SAR of the phenyl urea. To aid in this effort we were able to obtain an X-ray crystal structure of compound **2** bound to GPa. Herein we report the general binding interactions observed in the crystal structure, additional SAR of this series, as well as in vivo efficacy of these GPa inhibitors.

The X-ray crystal structure of compound **2** bound to GPa is shown in Figure 1 (view from solvent).[10] Compound **2** binds to GPa at the AMP regulatory site. Binding at this site can result in enzyme inhibition either by competing with the allosteric activator, AMP, or by stabilizing the inactive T conformation of the enzyme. The AMP binding site is partially solvent exposed at the dimer interface and lies along one of the protein's twofold axes of symmetry. This axis is the one on which the protein pivots as it shifts between the T (inactive) and R (active) state. Therefore binding at this site could be envisioned to block the shift between the T and R states.

The molecule forms a number of important hydrogen bonds to the protein as shown in Figure 2. The carboxylate of the amino-acid moiety forms a bidentate interaction with Arg310 of the phosphate-recognition site. The amide carbonyl forms a hydrogen bond with the NH2 of Gln71. The urea moiety forms two hydrogen bonds with the main-chain of the symmetry-related subunit (of the homo-dimer); (1) the urea NH with the carbonyl of Val40′ and (2) the urea carbonyl with the NH of Asp42′ (where the prime refers to residues from the symmetry-related subunit). These later interactions are similar to those observed for the acyl urea inhibitors previously reported.[11] More than a dozen other residues contribute to binding through van der Waals interactions. The lipophilic regions of the amino-acid moiety are surrounded by Phe196, the alkyl chain of Arg309 and Ala313. The polar end of Arg309 is flipped away from the binding site and is not participating in hydrogen bonding interactions with the ligand as is often observed in other crystal structures.[12] The naphthalene moiety is surrounded by residues Asp42′, Asn44′ and Val45′ as well as Ile68, Gln71, Gln72 and Tyr75. The urea phenyl ring is situated the deepest in the binding site and forms interactions with Trp67, Gln71, Thr240, Arg242, Asp227, Phe196, Lys41 and Arg193. Arg193 appears to be forming pi-stacking interactions with the ring and is in a conformation relative to the inhibitor that is different than that observed for the other reported AMP site binders.[11,12]

Examination of the ligand (compound **2**) in the crystal structure illustrates two interesting features of the binding confirmation. First is the potential for an internal hydrogen bond between the internal NH of the urea with the carbonyl of the amide. Second is the *s-cis* confirmation of the 2,4,6-dimethylphenylurea. In order to understand the low energy confirmation of the ligand we studied the model system shown in Figure 3 (shown in the *s-cis* configuration) with molecular mechanics (MacroModel, Schrodinger LLC) using the OPLS2005 force field and a constant dielectric of 4.0. The low energy conformation of this model includes an intra-molecular hydrogen bond between the amide carbonyl and the internal NH of the urea moiety. While the difference in energy between the *s-trans* and *s-cis* conformations of the un-substituted phenylurea analog was ~2.7 kcal/mol, the difference for the 2,6-dimethylphenylurea analog was ~0.5 kcal/mol. This significant difference is predicted to allow the 2,6-dimethyl substituted analogs to readily adopt the *s-cis* conformation and to bind to the protein with a minimal amount of strain. These features aid in the understanding of

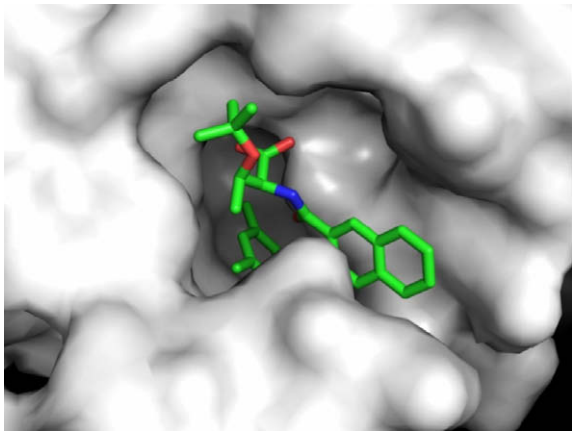

Figure 1. X-ray crystal structure of compound **2** bound to GP at the AMP site.

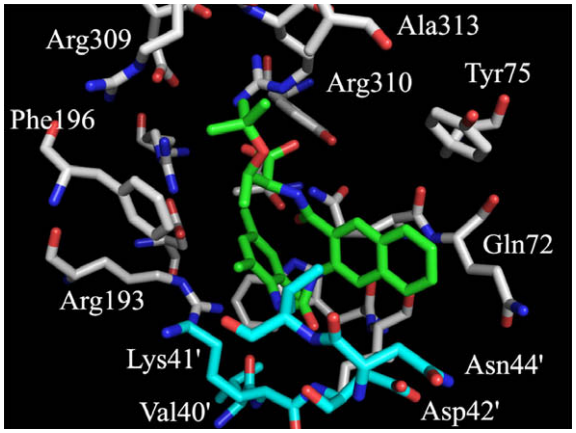

Figure 2. X-ray crystal structure of compound **2** bound to GP, showing key binding interactions. Prime residues reside on the symmetry-related subunit shown in blue.

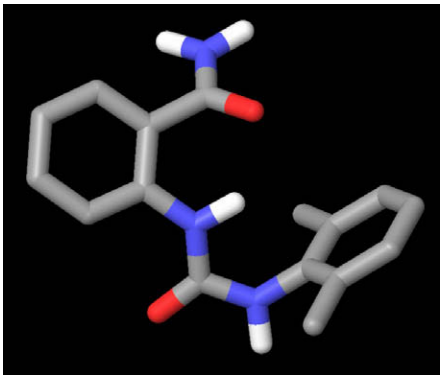

Figure 3. Model system used to study the effects of 2,6-dimethyl substitution on the stability of the *s-cis* conformation (shown). The *s-cis* configuration orients the urea carbonyl and NH toward the main-chain carbonyl and NH of Val40′ and Asp42′.

previously reported SAR for this series of compounds in which the 2,6-dimethylphenyl urea was greater than 100 times more potent than the 2-methylphenyl urea.[6]

From the crystal structure one can see that the naphthalene group binds in a narrow lipophilic channel, nearly ending at the solvent front. This interaction contributes significantly to the activity of this series of compounds since replacement of the naphthyl group with a phenyl results in a large loss of activity in at the enzyme assay (see Table 1).[13] From this structure one could envisage replacing the naphthyl group with a bi-aryl group, which would allow for easier introduction of diversity in this region of the molecule.

The general synthesis of these bi-aryl anthranilimides is shown in Scheme 1.[14] This synthetic pathway allows for easy variation of the outboard phenyl ring by employing various phenylboronic acids. As shown in Table 1 the naphthalene group can be replaced with substituted bi-phenyl groups with little change in activity. Unlike compound **2**, incubation of compound **9** with human liver microsomes in the presence of glutathione showed no evidence of formation of reactive metabolites via oxidation and addition to the bi-aryl ring system.[9] In addition to the enzyme inhibition assay the compounds were evaluated in a cell based assay to inhibit forskolin stimulated glycogenolysis.[15] Although potency in the cell assay does not track directly with enzyme inhibition potency, in general the more potent a compound is at the enzyme the more potent it will be in the cell assay. It is important to note that several of these compounds are reaching the lower limit of the enzyme assay and could be more potent than reported.[13]

Table 1
SAR of naphthyl replacements

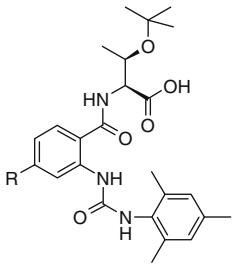

Compound	R	GPa inhibition IC_{50}[a] (nM)	GPa (cell)IC_{50} (nM)
3	H	542 (96)	1680
4	F	506 (25)	1820
5	Phenyl	10 (7)	126 (49)
6	4-MeOphenyl	3 (2)	34 (14)
7	3-MeOphenyl	8 (3)	109
8	2-MeOphenyl	28 (16)	353 (56)
9	3-Fluorophenyl	15 (4)	104 (19)
10	4-Fluorophenyl	7 (3)	88 (21)
11	3,4-Difluorophenyl	13 (6)	171 (24)

[a] Values are means of three experiments, standard error is given in parentheses.

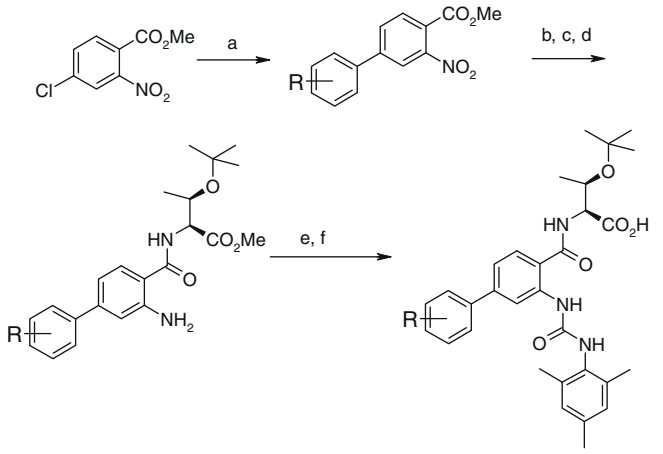

Scheme 1. General syntheses of compounds **5**–**11**. Reagents and conditions: (a) R-PhB$(OH)_2$, Pd$(Cy_3P)_2Cl_2$, CsF, CH_3CN, H_2O, 150 °C, 5 min, microwave; (b) LiOH, H_2O, MeOH, THF; (c) methyl *O*-(1,1-dimethylethyl)-L-threoninate hydrochloride, HATU, *i*PrNEt_2, DMF, rt; (d) H_2, 5% Pd/C, EtOH; (e) 2,4,6-Me_3PhNCO, pyr; (f) LiOH, H_2O, MeOH, THF.

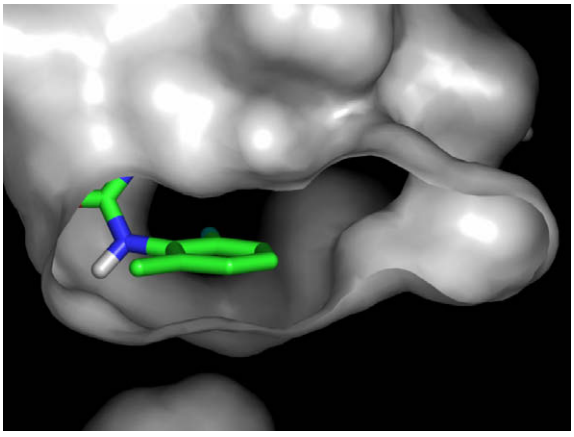

Figure 4. Crystal structure of compound **12**, showing the view of the lipophilic pocket off the 4 position on the phenyl urea.

We next turned to the SAR of the phenyl urea. In our previous paper, we reported improved potency of the 2,4,6-trimethylphenyl versus 2,6-dimethylphenyl urea.[7] The reason for this improvement is clear upon closer examination of the crystal structure (see Fig. 4). Off of the 4 position of the phenyl urea there appears to be a narrow pocket defined by residues Tyr155, Thr240, Arg242 and Arg310, which can accommodate the 4-methyl group. We wished to explore the boundaries of this pocket and therefore prepared the compounds listed in Table 2. Here we selected the less active 4-flourophenyl core as the test case so that the SAR of the 4 position of the phenyl urea ring can be delineated without reaching the lower limit of the assay. The general route to these compounds is shown in Scheme 2, in which the key bromide intermediate can be functionalized to give various sized alkyl groups via a palladium mediated coupling reaction and subsequent hydrogenation. For compound **16** the cyclopropyl ring was constructed via palladium mediated addition of diazomethane to the olefin of the allyl intermediate.[16]

Table 2
SAR of 4-alkyl phenyl urea

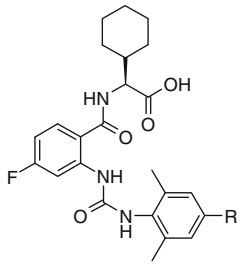

Compound	R	GPa inhibition IC_{50}[a] (nM)	GPa (cell) IC_{50} (nM)
12	H	1067 (230)	8260
13	Me	143 (23)	1026 (244)
14	Et	87 (23)	513
15	*n*-Pr	19 (10)	229
16	Cyclopropylmethyl	13 (7)	384
17	*n*-Butyl	49 (21)	716

[a] Values are means of three experiments, standard error is given in parentheses.

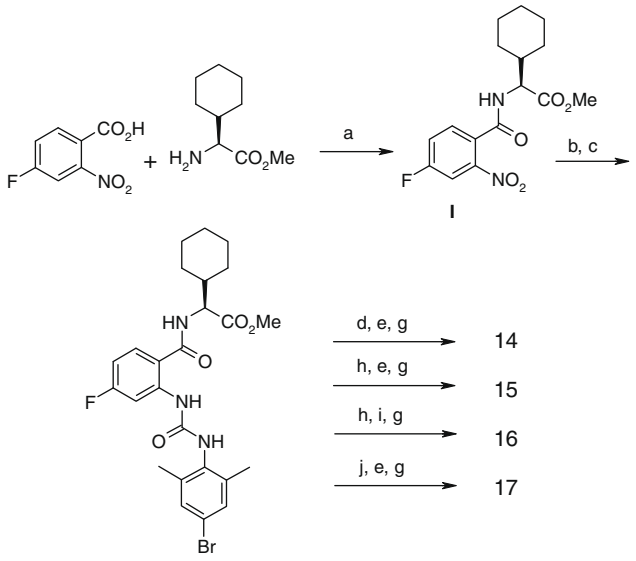

Scheme 2. General syntheses of compounds **14**–**17**. Reagents and conditions: (a) HATU, *i*PrNEt$_2$, DMF, rt, (b) H_2, 10% Pd/C, ethyl acetate; (c) 2,6-Me$_2$-4-BrPhNCO, pyr, rt; (d) vinyltributyltin, Pd(Ph$_3$P)$_4$, CH_3CN, 150 °C, 30 min, microwave; (e) H_2, Pd/C, ethyl acetate; (g) LiOH, H_2O, MeOH, THF; (h) allyltributyltin, Pd(Ph$_3$P)$_4$, CH_3CN, 150 C, 30 min, microwave; (i) CH_2N_2, Pd(acac)$_2$, Et_2O, CH_2Cl_2, −5 °C; (j) 2-[(1*E*)-1-buten-1-yl]-1,3,2-benzodioxaborole, Pd(Cy$_3$P)$_2$Cl$_2$, CsF, CH_3CN, H_2O, 150 C, 7 min, microwave.

As can be seen in Table 2 increasing the size of R from H to *n*-propyl results in an improvement in potency both at the enzyme as well as in the cell based assay. In this case there is a good correlation between enzyme potency and cell potency. When R is *n*-butyl there appears to be some loss of activity and this maybe approaching the limit of the pocket size. Incorporation of *n*-propyl and cyclopropylmethyl at the 4 position of the phenyl urea was also carried out with the *t*-butyl threonine head group in place as shown in Table 3 (synthetic scheme equivalent to Scheme 2 in which *t*-butyl threonine is used). Again in this series increased size at the 4 position of the urea results in improved potency in both the enzyme and cell assays. As reported earlier[7] the *t*-butyl threonine head group decreases CYP2C9 inhibition and this trend holds true when comparing the CYP2C9 activity of compounds **16** and **19** (data not shown).

Table 3
SAR of 4-alkyl phenyl urea with *t*-butyl threonine head group

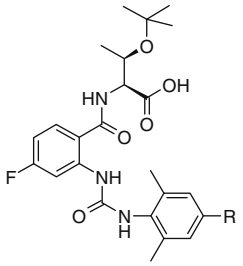

Compound	R	GPa inhibition IC_{50}[a] (nM)	GPa (cell) IC_{50} (nM)
4	Me	506 (25)	1820
18	*n*-Pr	10 (2)	147 (42)
19	Cyclopropylmethyl	4 (1)	133 (28)

[a] Values are means of three experiments, standard error is given in parentheses.

From Table 1 we know that replacement of the fluoro group of compound **4** with a phenyl group (compound **5**) results in a large increase in potency. Therefore we wished to prepare bi-phenyl compounds like **5–11** which also contain *n*-propyl and cyclopropylmethyl substitutions at the 4 position of the phenyl urea (compounds of Table 4). The synthesis of these compounds utilizes reactions shown in Schemes 1 and 2. Using a reaction sequence equivalent to that shown in Scheme 1, but employing 5-bromo-2-isocyanato-1,3-dimethylbenzene instead of the 2-isocyanato-1,3,5-trimethylbenzene gives the key bromo intermediate which can then be functionalized at the 4 position of the urea in a manner equivalent to that outlined in Scheme 2. As shown in Table 4 this gives compounds that are all within the limit of the enzyme inhibition assay,[13] but somewhat surprising is that these compounds do not show an increase in potency in the cell based assay compared to compounds **5–11**. It is possible that a lower limit in potency exist in this cellular assay due to cellular enzyme levels, although compound **6** (Table 1) would suggest it to be lower than 50 nM.

To further understand and differentiate the activity of these compounds we examined their ability to inhibit the glucose rise induced by iv administered glucagon in an in vivo rat model.[17] Compounds were dosed orally 2 h prior to the glucagon challenge and the data is reported as the % reduction (%*R*) in the glucose AUC

Table 4
Biphenyl compounds with 4-alkyl phenyl urea substitutions

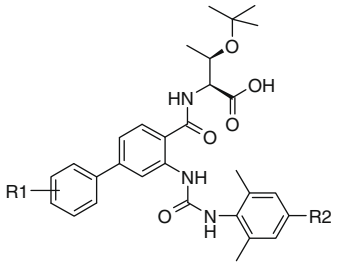

Compound	R1	R2	GPa inhibition IC_{50}[a] (nM)	GPa (cell) IC_{50} (nM)
20	3,4-F	*n*-Pr	7 (10)	181 (27)
21	4-OMe	*n*-Pr	4 (1)	135 (17)
22	3-F	*n*-Pr	4 (1)	156 (15)
23	3-F	Cyclopropylmethyl	3 (1)	145 (18)

[a] Values are means of three experiments, standard error is given in parentheses.

Table 5
Inhibition of glucagon induced glucose AUC in rats ($n = 4$)

Compound	GPa inhibition IC_{50} [a] (nM)	GPa (cell) IC_{50} (nM)	%*R* @ 5 mg/kg[b]	%*R* @ 2 mg/kg[b]
2	7 (2)	139 (41)	25	ND
9	15 (4)	104 (19)	32	10
19	4 (1)	133 (28)	36	22
23	3 (1)	145 (18)	65	62

Compounds were dose orally 2 h prior to the glucagon challenge.
[a] Values are means of three experiments, standard error is given in parentheses. ND = not determined.
[b] $p < 0.005$ for all.

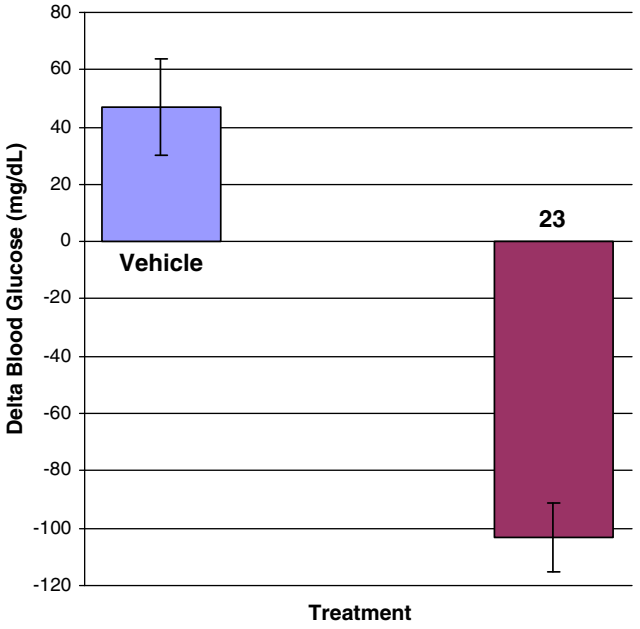

Figure 5. Effect on blood glucose in ob/ob mice by compound **23** dosed at 15 mg/kg compared to vehicle 3 h postdosing ($n = 10$).

for 20 min post glucagon treatment. As can be seen in Table 5 these compounds are able to inhibit the effect of glucagon, which is presumed to be via the inhibition of GP in the liver. It is of interest that although these compounds do not differ appreciably in their in vitro cell activity compound **23** which we would predict to be the most active based on the herein reported SAR is significantly more active in vivo. This could be due to a variety of factors, such as differences in pharmacokinetics,[18] tissue distribution (liver exposure) and enzyme inhibition in the in vivo system.

To further investigate the anti-diabetic effect of this series of compounds we evaluated the glucose lowering ability of compound **23** in a diabetic mouse model (ob/ob).[19] In this model fed ob/ob mice were orally dosed either with compound **23** (15 mg/kg) or vehicle and blood glucose was measured before dosing and 3 h later. As shown in Figure 5 compound **23** gave a robust response, lowering glucose levels 103 + 12 mg/dL whereas in the vehicle treated mice the glucose levels increase 47 + 17 mg/dL over the 3 h period ($p < 0.000001$).

In summary, we have described the key binding interactions and conformation of this series of anthranilamide based GPa inhibitors and by using the knowledge gained from the crystal structure we have expanded the SAR to deliver extremely potent molecules. Combining the best features of the SAR has yielded inhibitors which are able to inhibit GP in vivo at low doses as measured by a glucagon challenge test. In addition we have shown that a compound in this series can acutely lower glucose levels in a diabetic mouse model (ob/ob). In future publications, we will delineate the PK properties of these compounds as well as describe additional in vivo efficacy studies of this series of compounds.

References and notes

1. (a) Reinehr, T.; Schober, E.; Roth, C. L.; Wiegand, S.; Holl, R. *Horm. Res.* **2008**, *69*, 107; (b) Weiss, R.; Taksali, S. E.; Caprio, S. *Curr. Diab. Rep.* **2006**, *6*, 182; (c) Soltesz, G. *Diabetes Res. Clin. Pract.* **2006**, *74*, S9–S11.
2. (a) Ebbeling, C. B.; Pawlak, D. B.; Ludwig, D. S. *Lancet* **2002**, *360*, 473; (b) Hannon, T. S; Rao, G.; Arslanian, S. A. *Pediatrics* **2005**, *116*, 473.
3. (a) Kahn, S. E.; Haffner, S. M.; Heise, M. A.; Herman, W. H.; Holman, R. R.; Jones, N. P.; Kravitz, B. G.; Lachin, J. M.; O'Neill, C.; Zinman, B.; Viberti, G. *N. Eng. J. Med.* **2006**, *355*, 2427; (b) Monami, M.; Lamanna, C.; Marchionni, N.; Mannucci, E. *Diabetes Res. Clin. Pract.* **2008**, *79*, 196.
4. (a) Woerle, H. J.; Szoke, E.; Meyer, C.; Dostou, J. M.; Wittlin, S. D.; Gosmanov, N. R.; Welle, S. L.; Gerich, J. E. *Am. J. Physiol.* **2006**, *290*, E67; (b) Magnusson, I.; Rothman, D. L.; Katz, L. D.; Shulman, R. G.; Shulman, G. I. *J. Clin. Invest.* **1992**, *90*, 1323.
5. (a) Chen, L.; Li, H.; Liu, J.; Zhang, L.; Liu, H.; Jiang, H. *Bioorg. Med. Chem.* **2007**, *15*, 6763; (b) Birch, A. M.; Kenny, P. W.; Oikonomakos, N. G.; Otterbein, L.; Schofield, P.; Whittamore, P. R. O.; Whalley, D. P. *Bioorg. Med. Chem. Lett.* **2007**, *17*, 394; (c) Henke, B. R.; Sparks, S. M. *Mini-Rev. Med. Chem.* **2006**, *6*, 845; (d) Li, Y. H.; Coppo, F. T.; Evans, K. A.; Graybill, T. L.; Patel, M.; Gale, J.; Li, H.; Tavares, F.; Thomson, S. A. *Bioorg. Med. Chem. Lett.* **2006**, *16*, 5892. and references therein.
6. Evans, K. A.; Li, Y. H.; Coppo, F. T.; Graybill, T. L.; Cichy-Knight, M.; Patel, M.; Gale, J.; Li, H.; Thrall, S. H.; Tew, D.; Tavares, F.; Thomson, S. A.; Weiel, J. E.; Boucheron, J. A.; Clancy, D. C.; Epperly, A. H.; Golden, P. L. *Bioorg. Med. Chem. Lett.* **2008**, *18*, 4068.
7. (a) Sparks, S. M. et al *Bioorg. Med. Chem. Lett.* **2009**, *19*, 976; (b) Sparks, S. M. et al *Bioorg. Med. Chem. Lett.* **2009**, *19*, 981.
8. (a) Shultz, M. A.; Choudary, P. V.; Buckpitt, A. R. *J. Pharmacol. Exp. Ther.* **1999**, *290*, 281; (b) Buckpitt, A. R.; Warren, D. L. *J. Pharmacol. Exp. Ther.* **1983**, *225*, 8.
9. Castro-Perez, J.; Plumb, R.; Liang, L.; Yang, E. *Rapid Commun. Mass Spectrom.* **2005**, *19*, 798.
10. GP protein was engineered with an N-term fusion to a hexa his-tag followed by a TEV protease site and expressed in *Escherichia coli*. Cells were lysed and activated to immobilized metal affinity chromatography (IMAC). Fractions containing GP were pooled, diluted and subjected to anion exchange chromatography (Q Sepharose HP). Fractions containing GP were pooled and the enzyme was activated. TEV protease was used to remove the tag and the activated cleaved GP was activated to another round of IMAC. The GP in the IMAC flow through was concentrated for crystallography. Crystals were prepared similar to the method described by Rath et al. for the active conformation of glycogen phosphorylase (see Rath, V. L.; Ammirati, M.; LeMotte, P. K.; Fennel, K. F.; Mansour, M. N.; Denley, D. E.; Hynes, T. R.; Schulte, G. K.; Wasilko, D. J.; Pandit, J. *Mol. Cell* **2000**, *6*, 139). The crystallization method was modified to include the addition of 5.0 mM caffeine and 0.1 mM ligand to the protein solution 1 h prior to setting up the crystals. Crystals were frozen in liquid nitrogen directly from the drop and X-ray diffraction data was collected at 100 K using an ADSC Q210 detector on the Advanced Photon Source Beam line 17ID at Argonne National Labs. The structure was solved by molecular replacement using the program Amore from PDB entry 1em6. Refinement was carried out using Refmac and other CCP4 tools and the final model was built using the programs O and Coot.Compound **2** cocrystals diffracted to 1.80 Å in resolution with an *R*-merge of 8.7%. The final model was refined to an *R*-factor of 17.4% with a Free *R*-factor of 19.8%. Compound **12** cocrystals diffracted to 1.90 Å in resolution with an *R*-merge of 7.8%. The final model was refined to an *R*-factor of 15.3%, with a Free *R*-factor of 18.6%. Coordinates and statistics are available from the PDB using accession code 3DDS and 3DDW, respectively.
11. Klabunde, T.; Wendt, K. U.; Kadereit, D.; Brachvogel, V.; Burger, H.; Herling, A. W.; Oikonomakos, N. G.; Kosmopoulou, M. N.; Schmoll, D.; Sarubbi, E.; Von Roedern, E.; Schoenafinger, K.; Defossa, E. *J. Med. Chem.* **2005**, *48*, 6178.
12. Kristiansen, M.; Andersen, B.; Iversen, L. F.; Westergaard, N. *J. Med. Chem.* **2004**, *47*, 3537.
13. Inhibitors were tested for human liver glycogen phosphorylase enzymatic activity using a coupled kinetic fluorescence intensity assay. The change in fluorescence due to product formation was measured on a fluorescence plate reader (Molecular Devices SpectraMax M2) using a excitation wavelength of 560 nm and an emission wavelength of 590 nm. The hGPa enzyme IC_{50} values given in Tables 1–5 are average values of at least two replicates where standard deviations are noted, and were measured in the presence of glucose (10 mM). Due to the specific activity of the enzyme, a concentration of 10–15 nM glycogen phosphorylase is used in the assay. Therefore, inhibitors with IC_{50} determined to be < approximately 5 nM (K_d < enzyme concentration) cannot be accurately evaluated in this assay format. Inhibitors falling into this category may have IC_{50} significantly lower than the estimate. For further experimental details, see Evans, K. A.; Cichy-Knight, M.; Coppo, F. T.; Dwornik, K. A.; Gale, J. P.; Garrido, D. M.; Li, Y. H.; Patel, M.; Tavares, F. X.; Thomson, S. A.;

Dickerson, S. H.; Peat, A. J.; Sparks, S. M.; Banker, P.; Cooper, J. P. WO 2006/052722 A1.
14. All novel compounds were characterized by NMR and LCMS, and gave satisfactory results in agreement with the proposed structure.
15. This full curve assay was designed to detect the inhibition of glycogenolysis (glycogen breakdown) by test compounds. On the day before the assay the glycogen in HepG2 cells is pre-labeled by overnight inclusion of ^{14}C-glucose in the culture medium. To begin the assay, the cells are treated with test compounds, and glycogenolysis is stimulated by forskolin treatment for 60 min. The cells are then lysed and the radiolabeled glycogen in the cells is quantified. If a test compound inhibits glycogenolysis, the radiolabeled glycogen content of the cells will be greater than control (forskolin treated). The hGPa(cell) IC_{50} values given in Tables 1–5 are average values of at least two replicates where standard deviations are noted.
16. Ma, D.; Zhu, W. *J. Org. Chem.* **2001**, *66*, 348.
17. Jugular vein cannulated male CD rats (220–260 g) were received 1–2 days after cannulation, housed individually with free access to food and water for 4 days prior to the glucagon challenge (GC) studies. The rats were sorted by body weight into treatment groups (N = 4–5). Rats were dosed orally with vehicle (5% DMSO: 30% Solutol HS15: 20% PEG400: 45% 25 mM *N*-methylglucamine) or drug (0.1–15 ml/kg) 2 h prior to the glucagon challenge (GC). A time zero blood sample (0.4 ml) was collected for determination of glucose and the rats were dosed via the jugular vein with Sandostatin, 0.5 mg/kg, and glucagon, 10 μg/kg. Blood samples were collected after 10 and 20 min. Whole blood was allowed to sit at room temperature for 20 min and then centrifuged (3000*g*) to obtain serum. Serum levels of glucose were determined using an Olympus AU640™ clinical chemistry immuno-analyzer.
18. For compound **23**, rat PK (IV dosed at 1 mg/kg, PO dosed at 5 mg/kg); Cl = 15 mL/min/kg, $T_{1/2}$ = 2.3 h,%F = 27, PO C_{max} = 536 ng/mL).
19. ob/ob mice, Strain B6.V-Lep^{ob}/J Stock No. 000632 (Drasher, 1955) (6–7-wk-old) were housed 3–4/cage with free access to food and water for 1–2 wk. On the day prior to analysis, the mice were sorted by blood glucose (tail snip, glucometer) and body weight into treatment groups (N = 10 for drug, N = 20 for vehicle). On the following day, the mice were moved to the study room at 6:30 am, and allowed to acclimate for ~1 h. Basal fed glucose levels were measured by tail-nick and glucometer read and the mice were dosed with 10 ml/kg vehicle (5% DMSO: 30% Solutol HS15: 20% PEG400: 45% 25 mM *N*-methylglucamine) or drug, at 8 am. Blood glucose levels were measured again by tail-nick and glucometer at 11 am.